



Inhibited Spontaneous Emission of Quantum Dots Observed in a 3D Photonic Band Gap

M. D. Leistikow,^{1,2} A. P. Mosk,¹ E. Yeganegi,¹ S. R. Huisman,¹ A. Lagendijk,^{1,2} and W. L. Vos^{1,*}

¹*Complex Photonic Systems (COPS), MESA+ Institute for Nanotechnology, University of Twente, 7500 AE Enschede, The Netherlands*

²*FOM Institute for Atomic and Molecular Physics (AMOLF), 1098 XG Amsterdam, The Netherlands*

(Received 23 May 2011; published 3 November 2011)

We present time-resolved emission experiments of semiconductor quantum dots in silicon 3D inverse-woodpile photonic band gap crystals. A systematic study is made of crystals with a range of pore radii to tune the band gap relative to the emission frequency. The decay rates averaged over all dipole orientations are inhibited by a factor of 10 in the photonic band gap and enhanced up to $2\times$ outside the gap, in agreement with theory. We discuss the effects of spatial inhomogeneity, nonradiative decay, and transition dipole orientations on the observed inhibition in the band gap.

DOI: 10.1103/PhysRevLett.107.193903

PACS numbers: 42.70.Qs, 42.50.Pq, 78.47.jd, 78.67.Hc

In the field of cavity quantum electrodynamics (QED) it has been recognized that the nanoenvironment of a two-level quantum system may serve to tailor the fundamental light-matter interactions [1,2]. Of particular interest is the broadband and complete suppression of vacuum fluctuations in a three-dimensional (3D) photonic band gap, i.e., a frequency range for which light is forbidden for all wave vectors and all polarizations [3]. Such band gaps are expected in 3D photonic crystals, i.e., dielectric nanostructures with periodicities less than half the optical wavelength [4]. Anticipated cavity QED effects of band gaps include complete inhibition of spontaneous emission, photon-atom bound states, collective laserlike emission, and intriguing fractional decay [5–9].

To date, the cavity QED effects of 3D photonic band gaps on two-level light sources have only been studied in theory [5–9]. In these studies, one usually considers a single two-level source (or N identical ones) with ideal 100% quantum efficiency that is excited once at $t = 0$, and that is placed in a perfect and infinitely extended photonic crystal. Clearly, this idealized situation differs from real situations. Real sources are inhomogeneously broadened, have nonzero nonradiative decay, are repeatedly excited in time, and are embedded in photonic crystals of finite extent. Previous experiments on 3D photonic crystals were restricted to inverse opals with pseudogaps [10]; hence, the above predictions could not be addressed.

In this Letter, we perform a first experimental study of cavity QED effects on light sources inside real photonic crystals with a full 3D photonic band gap. To this end, we have developed silicon photonic crystals with a diamond-like structure that have broad band gaps [11]. We perform time-correlated single photon counting experiments on embedded semiconductor quantum dots. We observe broadband inhibition inside the photonic band gap and enhancement outside the gap. We find that the effects of spatial inhomogeneity, nonradiative decay, and transition dipole orientations are relevant in the band gap. Our results

allow a first experimental test of theoretical cavity QED predictions [5–9].

Silicon 3D inverse-woodpile photonic band gap crystals were fabricated by a CMOS-compatible method described in Ref. [12]. In brief, a 2D array of pores was etched in a silicon wafer by reactive ion etching, and a second orthogonal set of pores was etched after careful alignment to yield 3D crystals. Figure 1(a) shows a micrograph of a typical 3D crystal that compares well to the designed structure shown in Fig. 1(b). The cubic crystals have lattice parameters $a = 693$ and $c = 488$ nm ($a/c = \sqrt{2}$), and a range of pore radii ($136 < r < 186$ nm) to tune the band gap relative to the emission spectrum. The 3D crystals extend over $L^3 = 12 \times 12 \times 12ac^2$, which exceeds the Bragg attenuation length (see [13]) in every direction [14]. The good optical quality and high photonic interaction strength (see [15]) of our crystals are confirmed by optical reflectivity where intense and broad peaks are seen. The stop bands overlap for all probed directions and polarizations, which is an experimental signature of a photonic band gap [14].

Figure 1(c) shows the calculated band structure [16] for an infinitely extended inverse-woodpile crystal. A broad band gap appears in the frequency range where modes are forbidden for all wave vectors. Figure 1(d) shows the corresponding density of states (DOS). At low frequency the DOS increases quadratically similar to an effective medium. The DOS deviates from the parabola beyond reduced frequency 0.35, and vanishes between 0.478 and 0.504 in the photonic band gap.

To study emission from two-level sources, we immersed the crystals in a dilute suspension of PbS colloidal quantum dots in toluene [17]. The dots emit at photon energies between 0.8 and 0.9 eV including the telecom range (Fig. 4), and their transition dipole orientations sample all directions. We have measured time-resolved emission at three energies in the quantum dot spectrum: 0.828, 0.850, and 0.893 eV ($\lambda = 1500, 1460, 1390$ nm, respectively) at room temperature. Outside the crystals the dots

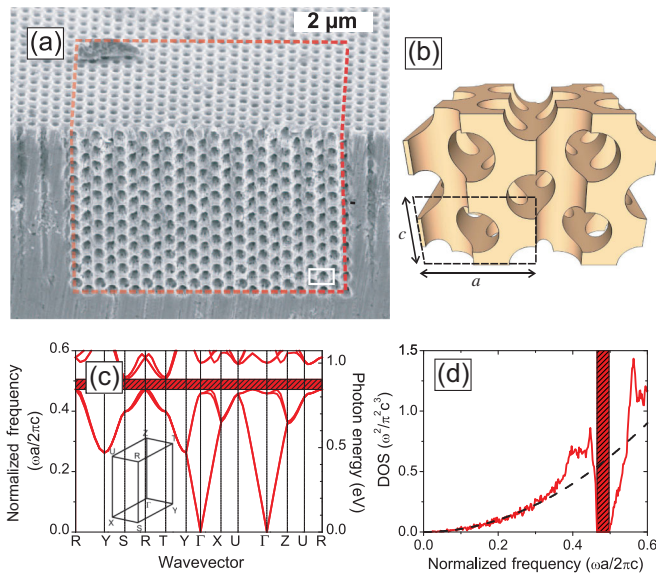


FIG. 1 (color). (a) Scanning electron micrograph of a 3D inverse-woodpile photonic crystal made from silicon. The 3D crystal is delimited by the dashed lines and consists of two perpendicularly etched sets of carefully aligned pores, surrounded by a 2D crystal. (b) Schematic image showing the positions and overlap of the pores, and unit-cell parameters a and c . (c) Band structure of an inverse-woodpile photonic crystal with pore radius 170 nm, $\epsilon = 12.1$ for silicon and $\epsilon = 2.25$ for toluene-filled pores. The band gap is indicated with the red bar. Inset: first Brillouin zone. (d) Density of states (DOS) per volume for the same crystal calculated with 10000 k points [16]. The DOS vanishes in the band gap. Dashed curve: quadratic behavior in the low frequency limit.

reveal single exponential decay with an energy-independent rate. By keeping the dots in suspension their photophysical properties remain stable for months, much longer than with dried dots in previous work [10].

The quantum dots were excited with short laser pulses at $\lambda = 532$ nm [17]. To minimize background from the suspension, light from the quantum dots was collected at 90° from the excitation beam by a detection objective with a high NA = 0.7 [see Fig. 2(a)], which does not affect the observed dynamics [17]. Light emitted by the quantum dots was resolved by a monochromator. To precisely align the crystal the excitation focus was scanned over the edge of the structure; see Fig. 2(b). We see a sharp transition from high (in suspension) to lower intensity in the crystal. In a scan performed on bulk silicon next to the crystal a sharp edge is also seen. Here the time-integrated intensity is about half of the intensity collected from the 3D photonic crystal. Hence about half of the intensity is emitted by quantum dots in the photonic crystal and the other half by dots in suspension. Therefore, a significant spontaneous emission signal originates from quantum dots in our photonic band gap crystals.

To precisely measure the arrival time of the emitted photons, time-correlated single photon counting was

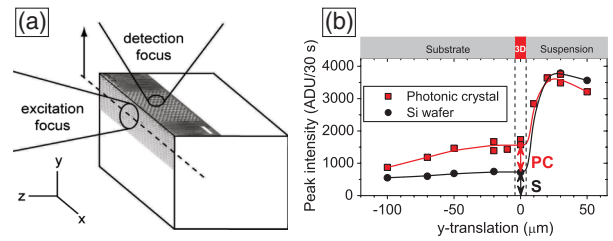


FIG. 2 (color). (a) Crystal position relative to excitation and detection foci. The coordinate system of the position scans is shown. (b) Peak intensity of quantum dots at 0.842 eV vs the y position of the excitation focus in an inverse-woodpile crystal (red squares) and near a silicon wafer (black circles), curves are guides to the eye. The signal below the 3D crystal stems from the nearby 2D crystal. The 3D crystal reveals twice as much signal as bulk silicon. *PC*, *S* (indicated by red and black arrows, respectively) are intensities measured at $y = 0$ that are input for time-resolved emission [Eq. (1)].

employed [17]. Since we perform experiments at relatively low photon energy in the near infrared to avoid silicon absorption, the detector darkcount is substantial and the quantum dot signal is relatively low. Therefore, we have collected for long times (hours) to obtain sufficient statistics, and carefully subtracted the background. Figure 3 shows time-resolved spontaneous emission for quantum dots in two different photonic crystals with pore radii $r = 170$ and 136 nm, compared to emission in suspension that serves as a reference. Emission outside the gap ($r = 136$ nm) decays faster than the reference, which illustrates that the excited-state lifetime of quantum dots is controlled by the photonic crystals. For the $r = 170$ nm crystal in the gap (0.893 eV) the emission is at short times (before ~ 500 ns) dominated by the relatively fast decaying suspension signal. Beyond this time, a much slower decay is apparent that reveals a strongly inhibited emission.

Interestingly Fig. 3 reveals that in the gap the histogram of photon arrival times decays monotonically in time to a vanishing intensity, in agreement with Ref. [6]; we do not detect signatures of fractional decay or oscillations predicted in Refs. [7–9]. For instance, based on Ref. [7] one expects photons to be emitted within an uninhibited lifetime (≤ 540 ns) followed by complete inhibition. In our experiments this would correspond to a decay curve that strongly deviates from exponential decay at times shorter than a lifetime. Because of the background suspension signal, at longer times only a contribution with the uninhibited rate would appear. We do not observe such phenomena in any of our data. A possible reason for this discrepancy may be that the predicted features are not robust to ensemble averaging. Other reasons could be the finite dynamic range (≤ 1.5 decades) in our work, the assumption of very large oscillator strengths in some models, or that theories predict excited-state population dynamics instead of photon arrival times while these two phenomena do not necessarily behave the same [18].

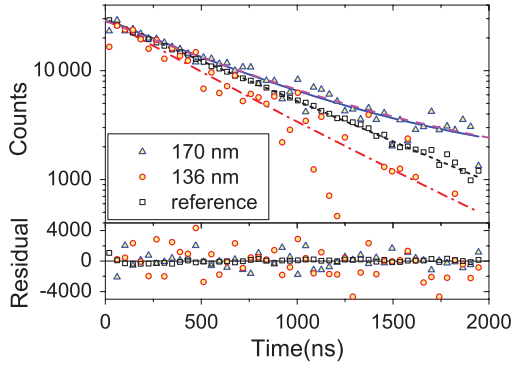


FIG. 3 (color). Time-resolved spontaneous emission measured on a quantum dot suspension for reference (black squares), a photonic crystal with pore radii 136 nm at 0.850 eV (red circles), and a crystal with $r = 170$ nm at 0.893 eV (blue triangles). Data rebinned to 40 ns steps. Blue, black, and red curves are bi-exponential models [Eq. (1)]. The magenta dashed curve is calculated from the LDOS distribution ([17]). Bottom panel: the residuals are random, indicating high quality fits.

Since the emission originates both from quantum dots in the crystal and in suspension, we model the time-resolved emission with a double-exponential (see Ref. [17,18]):

$$f(t) = I(S\gamma_S \exp(-\gamma_S t) + PC\gamma_{PC} \exp(-\gamma_{PC} t)). \quad (1)$$

Here γ_{PC} is the emission rate of quantum dots in the photonic crystal that we wish to obtain, and γ_S is the rate of dots outside the crystal that is separately measured to be $\gamma_S = 1.85 \mu\text{s}^{-1}$ (cf. Fig. 3). S and PC are relative factors fixed by scans of the detection focus [Fig. 2(b)], and only γ_{PC} and I are adjusted. Since the background is substantial compared to the signal, we have performed a maximum likelihood analysis of the time-resolved data, see the supplement [17]. Our model describes most data well, as is illustrated by residuals randomly distributed about 0 (Fig. 3 bottom), and by a goodness of fit χ_{red}^2 near unity. Some decay curves in the band gap could not be modeled and were excluded; while this is likely caused by experimental factors, it is also conceivable that Eq. (1) does not capture all physics in the band gap [17]. From Fig. 3 we obtain an emission rate $\gamma_{PC} = 3.1 \mu\text{s}^{-1}$ for the $r = 136$ nm crystal, a 1.5-fold enhancement. For the $r = 170$ nm crystal we obtain $\gamma_{PC} = 0.18 \mu\text{s}^{-1}$, corresponding to 10 \times inhibition. The resulting lifetime $T_1 = 5.5 \mu\text{s}$ is extremely long for quantum dots and indicates strongly shielded vacuum fluctuations, which is favorable for applications in quantum information processing [19].

Figure 4 (a) to (c) collects the emission rates measured on several crystals with a range of pore radii and hence gap frequencies. To investigate the inhibition in the photonic band gap range we plot the ratio γ_S/γ_{PC} . Since the quantum dots occupy a large fraction of the unit cell, they experience a local density of states (LDOS) averaged over a large part of the unit cell [20], which agrees well with the DOS for an infinite crystal [Fig. 1(c)]. For the

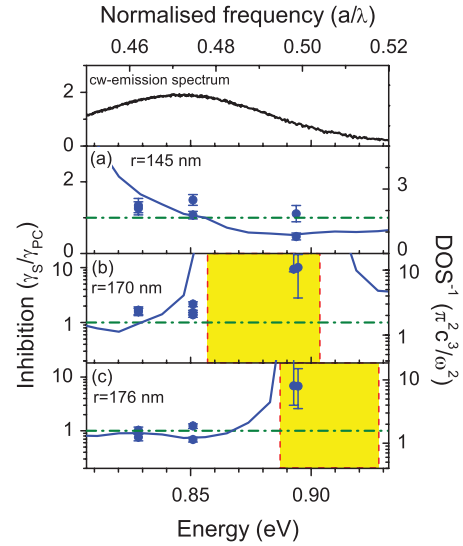


FIG. 4 (color). The top panel shows the quantum dots continuous-wave (cw) emission spectrum. (a) to (c): measured inhibition γ_S/γ_{PC} (open circles) versus photon energy for crystals with indicated pore radii. Different symbols are measurements on a same crystal on different days; data in the band gap (yellow) are displaced by 0.0005 eV for clarity. Horizontal lines indicate reference level. The calculated inverse density of states (DOS) are shown as curves.

145-nm crystal [Fig. 4(a)] the photon energy is higher than the band gap frequency. An enhanced emission rate up to 2 \times is observed with increasing photon energy, in agreement with the DOS. The 170-nm crystal [Fig. 4(b)] reveals up to twofold inhibition at frequencies just below the gap. Strikingly, a strong 10 \times inhibition is found at photon energies deep in the band gap where a low emission rate of $0.18 \mu\text{s}^{-1}$ is observed. Here the error bars are largest, as time-resolved emission is most sensitive to background when the emission rate is most strongly inhibited. The 176-nm crystal [Fig. 4(c)] also reveals a strongly inhibited emission rate in the frequency range that corresponds to the calculated band gap. A 7-fold inhibition is observed, in agreement with the results on the 170-nm crystal. The agreement of the observations on these two crystals is gratifying in view of the similar band gap width and center frequency.

Interestingly, the situation studied here leads to new physics since in real and finite 3D photonic band gaps the LDOS and the emission rate depend on depth z in the crystal. This contrasts to the calculated DOS curves in Fig. 4 that tend to infinite inhibition since they pertain to infinite crystal size. Based on theory [21] we expect the unit-cell-averaged LDOS to decrease exponentially with z in the band gap, see Fig. 5. In contrast, outside the gap the unit-cell-averaged LDOS varies only slightly with z from vacuum to the finite bulk value. In the gap, the LDOS for a finite crystal has a minimum at the center that is set by the crystal size L and by a decay length that we call ℓ_{LDOS} .

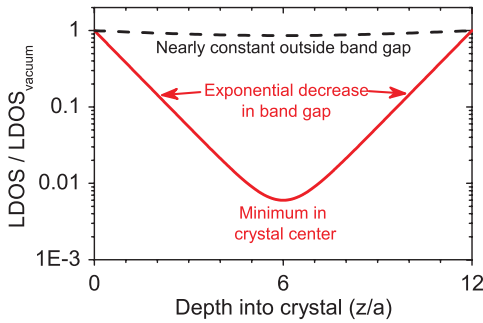


FIG. 5 (color). Unit-cell-averaged LDOS normalized to vacuum versus depth z in a finite photonic band gap crystal of extent $L = 12a$. In the gap the LDOS decreases exponentially with decay length $\ell_{\text{LDOS}} = 1.03a$ to a minimum 6×10^{-3} , as interpolated from Ref. [22] for $L = 12a$. Outside the gap the LDOS remains finite as in case of a pseudogap [10].

Interpolating the calculations of Ref. [22] to $L = 12a$, we estimate $\ell_{\text{LDOS}} = 1.03a$ and a maximum inhibition at the center of our crystals beyond $160\times$ (Fig. 5).

Spatial inhomogeneity has intriguing consequences: since the quantum dots experience a spatially dependent LDOS, we consider if the time-resolved emission curves are consistent with a distribution of emission rates. Indeed the z -dependent LDOS in Fig. 5 corresponds to a broad and asymmetric distribution of LDOS and thus of emission rates [17]. Using this distribution, we calculate an *ab initio* time-resolved emission curve that is in excellent agreement with the measured data, see Fig. 3. This supports the physical relevance of the length scale ℓ_{LDOS} in a band gap. In the measured time interval, the *ab initio* curve also agrees well with exponential decay. The difference between the two curves will be observable at much longer times than currently accessible, which requires greatly improved counting statistics. To take full advantage of the strong inhibition deep inside 3D crystals calls for completely different experimental approaches, viz., the probing of excited-state populations to directly verify the theoretical predictions [5–9]. We propose transient absorption as a probe of excited states that become more and more stable due to the shielding of the vacuum fluctuations in a 3D photonic band gap.

For any real light source we must also consider nonzero nonradiative decay. A time-resolved emission experiment yields a total rate that equals the sum of the radiative and nonradiative rates: $\gamma_{PC} = \gamma_{\text{rad}} + \gamma_{\text{nrad}}$. If γ_{rad} is strongly inhibited in a 3D photonic band gap, as is the case here, the rate γ_{PC} is minimal with a lower bound set by γ_{nrad} . While γ_{nrad} is not well known for our dots, we can estimate an upper bound from the maximum observed inhibition to be $\gamma_{\text{nrad}} \leq 0.18 \mu\text{s}^{-1}$, which is reasonable in view of data elsewhere [23]. In future γ_{nrad} may be reduced by cooling to low temperatures.

Finally, it is well known that the emission rate strongly depends on orientation of the transition dipole moment

[24]. Since our quantum dots are in suspension they sample all orientations; thus, the inhibition observed here is robust to orientation averaging. This is in contrast to recently observed inhibited emission in 2D photonic crystals [25], and nanowires [26] that concern dots with a particular orientation of the transition dipole moment.

We thank Léon Woldering, Hannie van den Broek, Willem Tjerkstra, and Frans Segerink for expert sample preparation, and Cock Harteveld for experimental help. This work is part of the research program of FOM that is financially supported by NWO. W. L. V. thanks NWO-Vici, and Smartmix Memphis.

Note added.—After our Letter was submitted, we learned of a study on spontaneous emission decay dynamics of nanocrystal quantum dots embedded in biotemplated titania photonic crystals with a diamond-based lattice [27]. This Letter reveals inhibition by about a factor of 5 in a range of strong stopgap overlap and $1.5\times$ enhancement near a band edge.

*w.l.vos@utwente.nl

www.photonicbandgaps.com.

- [1] S. Haroche, in *Fundamental Systems in Quantum Optics*, edited by J. Dalibard, J. M. Raimond, and J. Zinn-Justin (North Holland, Amsterdam, 1992), p. 767.
- [2] M. O. Scully and M. S. Zubairy, *Quantum Optics* (Cambridge University Press, Cambridge, 2001).
- [3] E. Yablonovitch, *Phys. Rev. Lett.* **58**, 2059 (1987).
- [4] J. D. Joannopoulos, S. G. Johnson, J. N. Winn, and R. D. Meade, *Photonic Crystals, Molding the Flow of Light* (Princeton University Press, Princeton, 2008).
- [5] S. John and J. Wang, *Phys. Rev. Lett.* **64**, 2418 (1990).
- [6] Z. Y. Li and Y. N. Xia, *Phys. Rev. A* **63**, 043817 (2001).
- [7] N. Vats, S. John, and K. Busch, *Phys. Rev. A* **65**, 043808 (2002).
- [8] X. H. Wang, B. Y. Gu, R. Z. Wang, and H. Q. Xu, *Phys. Rev. Lett.* **91**, 113904 (2003).
- [9] P. Kristensen, A. F. Koenderink, P. Lodahl, B. Tromborg, and J. Mørk, *Opt. Lett.* **33**, 1557 (2008).
- [10] P. Lodahl *et al.*, *Nature (London)* **430**, 654 (2004); I. S. Nikolaev *et al.*, *Phys. Rev. B* **75**, 115302 (2007).
- [11] K. M. Ho, C. T. Chan, C. M. Soukoulis, R. Biswas, and M. Sigalas, *Solid State Commun.* **89**, 413 (1994).
- [12] L. A. Woldering *et al.*, *Nanotechnology* **19**, 145304 (2008); J. M. van den Broek *et al.*, *Adv. Funct. Mater.* (to be published); R. W. Tjerkstra *et al.*, *J. Vac. Sci. Technol. B* (to be published).
- [13] S. Y. Lin and G. Arjavalingam, *Opt. Lett.* **18**, 1666 (1993); J. Huang, N. Eradat, M. E. Raikh, Z. V. Vardeny, A. A. Zakhidov, and R. H. Baughman, *Phys. Rev. Lett.* **86**, 4815 (2001).
- [14] S. R. Huisman, R. V. Nair, L. A. Woldering, M. D. Leistikow, A. P. Mosk, and W. L. Vos, *Phys. Rev. B* **83**, 205313 (2011).
- [15] W. L. Vos, R. Sprik, A. van Blaaderen, A. Imhof, A. Lagendijk, and G. H. Wegdam, *Phys. Rev. B* **53**, 16231 (1996).

- [16] S. G. Johnson and J. D. Joannopoulos, *Opt. Express* **8**, 173 (2001).
- [17] See supplemental material at <http://link.aps.org/supplemental/10.1103/PhysRevLett.107.193903> for theoretical background, details on experiments, data analysis, and model, and discussion on LDOS-distribution.
- [18] A. F. van Driel, I. S. Nikolaev, P. Vergeer, P. Lodahl, D. Vanmaekelbergh, and W. L. Vos, *Phys. Rev. B* **75**, 035329 (2007).
- [19] A. Imamoğlu, D. D. Awschalom, G. Burkard, D. P. DiVincenzo, D. Loss, M. Sherwin, and A. Small, *Phys. Rev. Lett.* **83**, 4204 (1999).
- [20] R. Sprik, B. A. van Tiggelen, and A. Lagendijk, *Europhys. Lett.* **35**, 265 (1996).
- [21] A. A. Asatryan, K. Busch, R. C. McPhedran, L. C. Botten, C. Martijn de Sterke, and N. A. Nicorovici, *Phys. Rev. E* **63**, 046612 (2001).
- [22] K. Ishizaki, M. Okano, and S. Noda, *J. Opt. Soc. Am. B* **26**, 1157 (2009).
- [23] M. D. Leistikow *et al.*, *Phys. Rev. B* **79**, 045301 (2009).
- [24] W. L. Vos, A. F. Koenderink, and I. S. Nikolaev, *Phys. Rev. A* **80**, 053802 (2009).
- [25] A. Kress, F. Hofbauer, N. Reinelt, M. Kaniber, H. J. Krenner, R. Meyer, G. Böhm, and J. J. Finley, *Phys. Rev. B* **71**, 241304(R) (2005); D. Englund, D. Fattal, E. Waks, G. Solomon, B. Zhang, T. Nakaoka, Y. Arakawa, and J. Vuckovic, *Phys. Rev. Lett.* **95**, 013904 (2005); M. Fujita, S. Takahashi, Y. Tanaka, T. Asano, and S. Noda, *Science* **308**, 1296 (2005).
- [26] J. Bleuse, J. Claudon, M. Creasey, N. S. Malik, J.-M. Gerard, I. Maksymov, J.-P. Hugonin, and P. Lalanne, *Phys. Rev. Lett.* **106**, 103601 (2011).
- [27] M. R. Jorgensen, J. W. Galusha, and M. H. Bartl, *Phys. Rev. Lett.* **107**, 143902 (2011).